

Taylor ex bg

GRAVITATIONAL CONSTANT MEASUREMENT USING A FOUR-POSITION PROCEDURE

O.V. Karagioz¹, V.P. Izmaylov[†] and G.T. Gillies[‡]

[†] Tribotech Research and Development Company, 5-12 Pyrieva St., Moscow 119285, Russia

[‡] Department of Mechanical, Aerospace and Nuclear Engineering,
University of Virginia, Charlottesville, Virginia 22903-2442, USA

Received 28 April 1998

A new determination of the Newtonian gravitational constant is reported. A modified and improved version of a torsion balance was used, in which an automated, motorized mechanism moves the attracting masses between fixed, well-determined points on ruled holders. Careful damping of the pendulum modes of the suspension system eliminated some parasitic modes of oscillation, but microseisms still restrict the precision of the measurement. After many series of runs, a value of $G = (6.6729 \pm 0.0005) \cdot 10^{-11} \text{ N} \cdot \text{m}^2/\text{kg}^2$ was the final result.

Измерение гравитационной постоянной с четырехпозиционной схемой фиксации
О.В. Карагиоз, В.П. Измайллов, Дж.Т. Гиллис

Приведены результаты измерений гравитационной постоянной, выполненные с помощью вакуумированных крутильных весов, при фиксации притягивающих масс на четырех позициях. Демпфирование маятниковых колебаний весов позволяет избавиться от некоторых паразитных мод, однако точность измерения остается ограниченной из-за воздействия микросейсм. Получено значение $G = (6.6729 \pm 0.0005) \cdot 10^{-11} \text{ Н} \cdot \text{м}^2/\text{кг}^2$.

1. Introduction

A refined version of a torsion balance with a classical vertical suspension fibre has been used to make a new series of measurements of the absolute value of the Newtonian gravitational constant G . As is often the case with such systems, a high sensitivity of the balance made it possible to carry out measurements using small test bodies. The measurements were made at several different mass separations, all of the order of 10 cm, a range which has historically been of interest to those searching for violations of the weak equivalence principle. Several other measurements of G have also been reported recently at both these and much larger inter-mass spacings [1] and, taken collectively, they are all of great interest in testing the precision of the inverse square law of gravitation over a wide range of mass separations. The presently recommended value of G is $(6.6729 \pm 0.00085) \cdot 10^{-11} \text{ N} \cdot \text{m}^2/\text{kg}^2$ as established during the 1986 CODATA adjustment of the fundamental constants [2]. This value is based on the result obtained by Luther and Towler [3] but includes a slightly larger uncertainty to reflect the values obtained by Pontikis [4] and Sagitov et al. [5]. A new value

of G will be established by CODATA once the new readjustment of the fundamental constants, presently underway, is completed. It will likely reflect the recent values of G reported by groups in New Zealand [6], Germany [7,8], Switzerland [9], the USA [10] and elsewhere (see Ref. [1] for a comprehensive discussion of many contemporary experiments). In what follows, we describe several design features of the latest version of an apparatus used in the ongoing redeterminations of the gravitational constant that have been carried out in Moscow over the past 25 years. Partial descriptions of some of the refinements made to the apparatus during this time have been presented in earlier papers [11, 12, 13].

2. Experimental arrangement

2.1. General features of the apparatus

There are several unique features of the apparatus that makes up this measurement system shown schematically in Fig. 1. With reference to that diagram, the torsion balance itself is housed in the vacuum chamber, 1. It is equipped with a magnetic damper, 3, whose rotary component is also separately acted on by a magnetic coupling, 2, used to adjust the equilibrium offset angle of the suspension fibre. The damper/coupling

¹ e-mail: irtrib@cityline.ru

² e-mail: gtg@unix.mail.virginia.edu

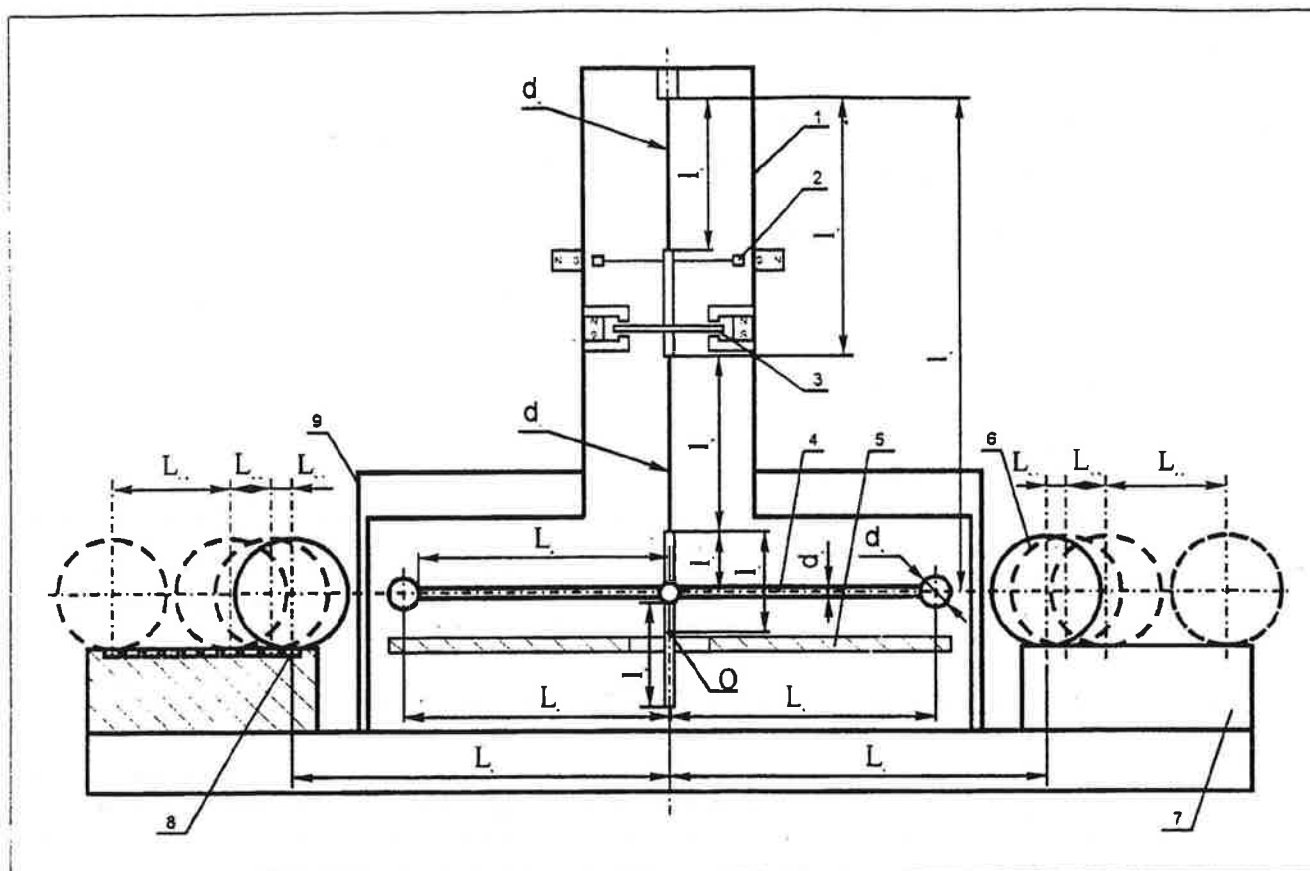


Figure 1: Diagram of the instrument: 1 — vacuum chamber; 2 — ferromagnetic masses fitted to the ends of the beam; 3 — aluminium disk; 4 — working body of the balance; 5 — copper plate; 6 — attracting ball masses; 7 — stationary rule; 8 — round holes; 9 — magnetic screen; d_1 , d_2 , d_3 , d_4 are diameters of the suspension string of the working body, of the auxiliary suspension string, of the beam loads and of the beam, respectively.

arrangement is suspended at a distance l_4 below the fibre's upper abutment point at the top of the vacuum chamber. The rotor of the damper is an aluminum disk positioned within the gaps of the pole pieces of two permanent magnets. The coupling consists of a beam with a ferromagnetic mass at both ends and a permanent magnet that acts on each mass. The magnets are located on the outer surface of the vacuum chamber.

The parameters of the torsion balance are given in Tables 1 and 2, with the corresponding distances and diameters indicated in Fig. 1. There is a round copper plate, 5, positioned below the beam, 4, which carries the test masses of the balance. As discussed below, the plate is part of the capacitive coupling mechanism used to anneal the suspension fibre. This plate is attached to the bottom of the vacuum chamber by three ceramic standoffs. An aluminum guide-rod extends downward from the underside of the beam and passes without contact through a centring hole in the copper plate. The chamber is evacuated by a 100 l/s ion discharge pump (not shown in Fig. 1). A 1-mm thick permalloy magnetic shield, 9, surrounds the chamber. The per-

meability of the shield in weak fields was maximized by annealing it in wet hydrogen at 1100° C for one hour.

The spherical attracting masses, 6, can be located at any of the positioning stations, 8, along the length of the stationary rules, 7. (A detailed schematic diagram of this arrangement is shown in Fig. 2.) One measurement scheme that makes use of this arrangement is the "four-position procedure" shown in Fig. 1. In this case the apparatus is used in the "symmetric mode" employing two attracting masses located at opposite sides of the vacuum chamber. The attracting masses are initially placed at points on the rules at a distance L_1 from the beam rotation axis. They are then moved to their second positions at a distance

$$L_2 = L_1 + L_{21}, \quad (1)$$

then thirdly to

$$L_3 = L_2 + L_{32}, \quad (2)$$

and finally to

$$L_4 = L_3 + L_{43}. \quad (3)$$

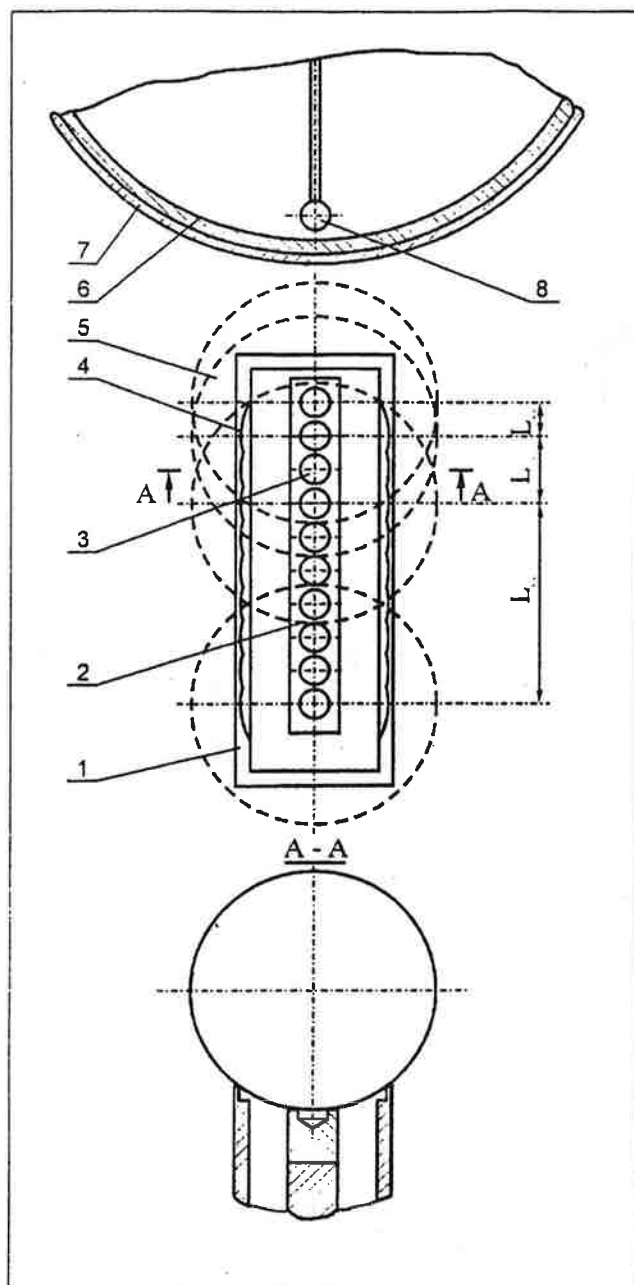


Figure 2: Diagram of the unit for moving and fixing the attracting ball masses: 1 — cut rule; 2 — stationary rule; 3 — round holes of the stationary rule; 4 — sectors of round holes of the cut rule; 5 — attracting mass; 6 — vacuum chamber wall; 7 — magnetic screen; 8 — spheric load of the beam.

In this scenario, used with rules having 10 positioning stations,

$$L_{43} = 3L_{32} = 6L_{21}. \quad (4)$$

Other measurement strategies can also be implemented with this system, including the use of an "asymmetric mode," where only one attracting mass is employed. In this case, the rule has 15 positioning stations, thus

allowing L_{43} to be larger than it is in the symmetric-mode arrangement.

An optoelectronic angular displacement transducer monitors the movement of the suspended beam. This system, shown schematically in Fig. 3, produces data that are read into files in a laboratory computer and then encoded, stored and processed by customized programs. Reconversion of the data back into the machine code can also be done to check the encoded files for any translation errors that might arise during the acquisition and formatting processes.

2.2. Operational characteristics

The torsion balance has simple-pendulum degrees of freedom [14], but the eddy currents induced in the disk of the damper, 3, attenuate the amplitude of the pendular oscillations of the swinging beam, 4. The suspension system and the beam assembly are designed to minimize the non-torsional oscillation frequencies of the beam, and the convergence of the highest frequency mode with those at lower frequencies works to enhance the damping efficiency of the parasitic degrees of freedom.

The plate, 5, is used for thermal treatment, in vacuo, of the suspension fibre of the balance. A high frequency (about 10 MHz) voltage is applied to the suspension fibre through a current lead. The current takes its path through the capacitance formed by the plate (which serves as an antenna) and the suspended mass. The annealing process decreases the drift of the suspension's equilibrium position and the damping factor.

With reference to Fig. 2, electric motors with speed reducers and crank mechanisms are used to move the "slotted gauges", 1. These are special rules that have spherical sectors machined out so that the attracting masses, 5, can be lifted by the slotted gauges from one of the round positioning holes, 4, in the stationary rules, 2, and moved to another. The start-time of the motor is specified by an electronic counter; the particular displacement program for a given mass and the stop-time of the motor are specified by push-button microswitches. When the displacement cycle is complete, the slotted gauges return to their initial position.

As described above, and shown in Fig. 3, the angular displacement transducer is an optical lever. The optical source, 1, in the lever consists of an incandescent lamp and condensing and imaging lenses, and forms a vertical stripe of light that is incident on the mirror, 2, mounted on the balance beam. After reflection from the mirror, the light falls between two photodiodes, 3, that constitute the lever's detector. The electric signals from the photodiodes drive a thresholding comparator, 4, which amplifies them and converts them into square pulses. The resulting wavetrains are monitored by a frequency meter, 5, that measures the time intervals between the pulses. The results of the time interval

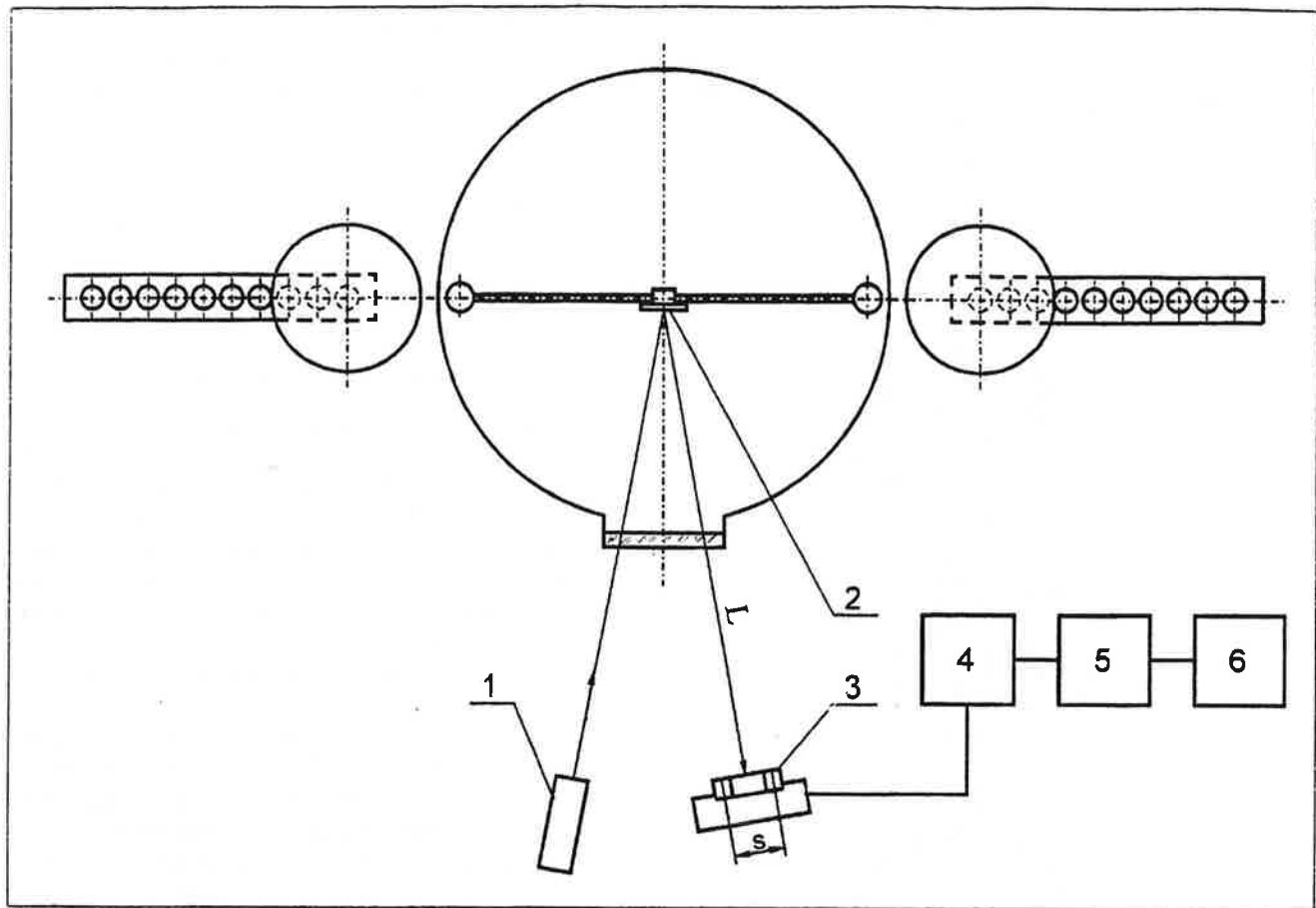


Figure 3: Diagram of the optoelectronic indication system: 1 — source of light; 2 — reflecting mirror; 3 — photodiodes; 4 — threshold device; 5 — frequency meter; 6 — transducer.

measurements are recorded by a data logger, 6, and also sent to a numerical printer, 7, for archiving.

Eight time intervals are measured between each successive start-cycle of the motor that moves the slotted gauges. The first two intervals carry systematic uncertainties due to the displacement process for the attracting masses. Among the other six, a group of 5 intervals is chosen: three long ones (t_{1i} , t_{3i} , t_{5i}) and two short ones (t_{2i} and t_{4i}). In our strategy, the sum of four selected time intervals is equal to the period of one anharmonic oscillation, T_i . The measurement of five intervals makes it possible to determine the values of two successive periods of nominal size T_i which are displaced in time by an amount t_{1i} . The final values of the oscillation period and amplitude of the balance when the centre of mass of the attracting sphere is held in the i -th position are labelled T_i and φ_{0i} . They are calculated by the formulae

$$T_i = 0.5(t_{1i} + t_{5i}) + t_{2i} + t_{3i} + t_{4i}, \quad (5)$$

$$\varphi_{0i} = \frac{c_3}{c_2 \sin[\pi(t_{2i} + t_{4i})/c_2 T_i]}, \quad c_3 = \frac{s}{2L} \quad (6)$$

where $c_2 = 1$ for an asymmetric procedure (a measurement with one attracting mass) and $c_2 = 2$ for a syn-

metric procedure (a measurement with two attracting masses); c_3 is a constant of the optical system. It is numerically equal to $s/2L$ where, as shown in Fig. 3, s is the spacing between the photodiodes in the detector assembly, and L is the distance from the photodiodes to the mirror, i.e., the length of the "lever arm."

Numerical data obtained from the period and amplitude measurements are used with the metrological constants and parameters of the apparatus in a set of difference equations that yield the values of the gravitational constant according to the algorithm explained in detail in [13]. The general principle of the measurement is one of taking the difference in the inverse squares of the measured oscillation periods before and after the displacement of the attracting masses by the slotted gauges. The technique is somewhat similar to the standard method of determining G by measuring the oscillatory period of a torsion pendulum with the attracting masses in "near" and "far" positions, or in quadrature positions (although the geometry of displacing the attracting masses is strictly along a single straight line in our case).

Table 1. Torsion balance specifications

| N | d_1 , μm | d_2 , μm | m_1 , g | m_2 , g | m_3 , mg | L_5 , cm | L_6 , cm | J , g cm^2 | c_1 , s/rad^2 |
|-----|--------------------------|--------------------------|--------------|--------------|---------------|---------------|---------------|--------------------------|-----------------------------|
| 1 | 8 | 25 | 0.9420 | 1.6575 | 230 | 11.8514 | 11.5500 | 338.397 | 790 |
| 2 | 6 | 15 | 0.9420 | 1.6575 | 171 | 11.8514 | 11.5500 | 338.397 | 100 |
| 3 | 10 | 25 | 1.5916 | 1.6575 | 171 | 11.9102 | 11.5500 | 525.429 | 12 |

Notations: N is the number of the type of the torsion balance; d_1 — diameter of the suspension fibre, d_2 — diameter of the auxiliary suspension fibre, m_1 — mass of the beam load; m_2 — mass of the beam, m_3 — mass of the rod attached to the centre of the beam; L_5 — the distance between the centre of mass of the beam load and the rotation axis; L_6 — the beam arm length; J — moment of inertia of the working body; c_1 — the period correction factor introduced when the balance oscillations amplitude changes due to the gravitational field gradient.

Table 2. Additional parameters of the torsion balances

| N | T s | m mg | m mg | l_0 mm | l_1 mm | l_2 mm | l_3 mm | l_4 mm | l_5 mm | l_6 mm | d_3 mm | d_4 mm |
|-----|----------|-----------|-----------|-------------|-------------|-------------|-------------|-------------|-------------|-------------|-------------|-------------|
| 1 | 2077 | 3999 | 996.05 | 20 | 23 | 221 | 296 | 262 | 537 | 150 | 6.017 | 1.8 |
| 2 | 3731 | 3972 | 996.05 | 20 | 21 | 227 | 295 | 261 | 542 | 108 | 6.017 | 1.8 |
| 3 | 1783 | 5254 | 959.25 | 20 | 21 | 227 | 295 | 261 | 542 | 108 | 7.165 | 1.8 |

Notations: T is the balance oscillation period; m — mass of the working body, m — mass of the intermediate body suspended from the auxiliary thread; l_0 — separation of the bottom point of the suspension from the beam axis; l_1 — separation of the lower point of suspension from the point O (centre of mass), l_2 — length of the suspension fibre, l_3 — separation between the upper fastening points of the main and auxiliary suspension fibres, l_4 — length of the auxiliary suspension fibre, l_5 — separation of the top fastening point of the auxiliary suspension string from the beam axis, l_6 — length of the rod which decreases the oscillation frequency, d_3 — diameter of the beam loads, d_4 — diameter of the beam.

Table 3. Results of measurements

| File | N | N_1 | M , g | L_1 , cm | L_2 , cm | L_3 , cm | L_4 , cm | $G \cdot 10^{11}$, Nm^2/kg^2 | σ/G , ppm |
|--------|-----|-------|------------|---------------|---------------|---------------|---------------|--|---------------------|
| 850419 | 1 | 911 | 7975.198 | 19.2115 | 21.2090 | 25.2067 | 47.2110 | 6.6730 | 90 |
| 850629 | 1 | 527 | 7975.198 | 19.5080 | 21.5055 | 25.5035 | 47.5078 | 6.6730 | 65 |
| 851211 | 1 | 701 | 7975.198 | 19.3937 | 21.3914 | 25.3889 | 47.3932 | 6.6730 | 64 |
| 860326 | 1 | 5050 | 4287.347 | 18.5920 | 20.5901 | 24.5881 | 46.5924 | 6.6730 | 43 |
| 870104 | 2 | 258 | 4287.347 | 18.2922 | 19.6909 | 22.4901 | 30.8884 | 6.6732 | 140 |
| 870303 | 2 | 1064 | 4859.959 | 18.3361 | 19.7361 | 22.5346 | 30.9329 | 6.6729 | 45 |
| 870714 | 2 | 150 | 4859.959 | 18.3361 | 19.7361 | 22.5346 | 30.9329 | 6.6729 | 90 |
| 870722 | 2 | 829 | 4287.347 | 18.3387 | 19.7387 | 22.5374 | 30.9357 | 6.6730 | 26 |
| 880802 | 3 | 1046 | 4859.959 | 18.5078 | 19.9072 | 22.7069 | 31.1052 | 6.6727 | 53 |
| 880805 | 3 | 1597 | 4282.375 | 18.5069 | 19.9063 | 22.7056 | 31.1039 | 6.6729 | 27 |
| 890309 | 3 | 2255 | 4282.375 | 18.5446 | 19.9439 | 22.7433 | 31.1416 | 6.6730 | 23 |
| 890606 | 3 | 396 | 4282.375 | 18.5469 | 19.9461 | 22.7455 | 31.1438 | 6.6729 | 33 |

Notations: N is the amount of G_{ij} in a given data file; M — the mass of attracting balls taking into account the air forced out; L_i — separation between the centre of mass of a ball and the rotation axis.

Table 4. Evaluation of measurement error

| Source of error | Presumed error | $\Delta G/G$, ppm |
|---|---|--------------------|
| Separation $L_{2,1}$ | 1 μm | 65 |
| Separation $L_{3,2}$ | 1 μm | 6 |
| Moment of inertia | $2 \cdot 10^{-3} \text{ g} \cdot \text{cm}^2$ | 6 |
| Masses of beam loads | 0.01 mg | < 1 |
| Mass of beam | 0.01 mg | < 1 |
| Mass of attracting body | 20 mg | 4 |
| Amplitude of oscillations | 0.01 % | 3 |
| Coefficient c_1 | 10 % | 3 |
| Oscillation periods T_i | 0.5 ms | 10 |
| Vertical displacement h | 100 μm | 2 |
| Horizontal deviation about the equilibrium line of the beam | 3 μm | < 1 |
| Magnetic interaction | | < 1 |
| Microseisms | | 40 |
| Total error | | 78 |

3. Measurement procedure and use of the apparatus

After the evacuation of the balance and the annealing of the suspension fibre, the final adjustment of the apparatus takes place to prepare it for work. The equilibrium position of the balance is set within the torsion head. The stationary rules are located so as to provide a position of stable torsional equilibrium when an attracting mass is displaced from one point to another. The horizontal deflection of the beam along the direction perpendicular to the equilibrium axis is fixed with an uncertainty of no more than 1 μm . (Adjustment of the suspended mass along the vertical direction is carried out before evacuation of the balance.)

3.1. Variants of the instrument design

The instrumentation can be employed in one of two fundamentally different modes. In the first variant only one attracting mass is used. As mentioned above, this design is called "asymmetric". In the other variant two attracting masses are placed on opposite sides of the beam, and this is termed the "symmetric" case. In the asymmetric case, the stationary rule had 15 round holes in it, each of them 15 mm in diameter. In the symmetric case the rules had only 10 holes, each one 13 mm in diameter. By having several different measurement positions at which the attracting masses could be located, one can implement a method of determining the gravitational constant by equalizing all the values of individual measurements, G_{ij} , made at various combinations of the positions of the attracting masses [13,15,16].

3.2. Measurement procedure

During an automated sequence of measurements the attracting masses are displaced by the electric motor system from position i to j . The data were at first taken using only the asymmetric design. Later, after the instrumentation was upgraded, the data were also taken using the symmetric scheme. In one of its versions, the attracting masses were first located in the "extreme" position (i.e., farthest out on the stationary rules). Then the motorized drive would be activated to reverse their locations (i.e., move them to the innermost position on the stationary rules), and they would be cyclically displaced between these positions thereafter.

4. Results

The results of many series of automated measurements are shown in Table 3. The calculations were performed using the procedure outlined above and discussed in detail elsewhere [13,16]. The numbers in the first column denote the date (year, month, day) of the beginning of that particular series of measurements. The last column gives the ratio σ/G where σ is the root-mean-square (rms) uncertainty of the mean value of G in the data file under consideration. Until 1986 the experiments were carried out using the asymmetric procedure and Balance $N = 1$. (See Table 1 for the parameters of the experimental arrangements for Balance $N = 1, 2, 3$.) This setup made it possible to maximize the displacement range of the attracting mass. The symmetric design was used with other experimental arrangements, viz., Balance $N = 2$ in 1987 and Balance $N = 3$ from 1988 onward. The following attracting masses were used in the experiments: a brass mass of 121.98 mm in diameter ($M = 7975.198 \text{ g}$), a bronze mass of 101.6 mm in diameter ($M = 4859.959 \text{ g}$), and masses made of bearing steel that were also 101.6 mm in diameter. The measurements were carried out in a thermostated enclosure that maintained the apparatus at a temperature of $(23.0 \pm 0.1)^\circ\text{C}$.

In the course of the experiments we have observed a time drift in the value of G of up to $\pm 0.1\%$. Incorporation of the magnetic damper made it possible to decrease the effect of microseisms. So the observed drift is most likely due to some as yet unidentified instrumental destabilizing factor. We will be exploring the size and meaning of this aspect of our observations in an forthcoming article devoted to that topic. Taking into consideration the statistical weight of each experiment, which is proportional to the ratio G/σ , and the main sources of measurement uncertainty listed in the error budget presented in Table 4, we find

$$G = (6.6729 \pm 0.0005) \cdot 10^{-11} \text{ N} \cdot \text{m}^2/\text{kg}^2.$$

5. Conclusions

The result obtained here is in agreement with several previous findings, including those obtained by Luther and Towler [3] and Karagioz et al. [16]. The main source of uncertainty in the measurements is that due to the determination of the spacing between the two "near" positions of the attracting masses, which is about 1 μm .

The experience accumulated with the use of this apparatus over many years suggests that the microseisms indeed affect the results of the measurements. Moreover, the size of the uncertainty they introduce is the most difficult component of the error budget to either determine or predict. The basic technique for diminishing the uncertainty introduced by the microseisms involves the design and installation of a highly efficient magnetic damper. Some of the previous torsion balance determinations of G were made without such a device aimed at damping the pendulum oscillations in the suspension system [5, 15]. In the subsequent work [16], however, the availability of an appropriate damping mechanism made it possible to reduce the measurement uncertainty. Although a damping mechanism was used by Long [17], the scale dependence of G which was reported in that work (and which subsequently motivated many other early experimental tests of the inverse square law) could conceivably have arisen from inadequate damping of the parasitic modes. In the present work, the efficiency of the damper was enhanced by extending the length of the auxiliary suspension fibre as well as by increasing the moment of inertia of the suspended body relative to the axis of the beam. Cyclic repositioning of the attracting masses reduced all the uncertainties associated with low-frequency drifts of any kind to a minimum. But even having undertaken all these measures, the effects of the microseisms still could not be eliminated completely. To further approach this goal, it will most likely be necessary to continue improving the design of the damping system. A decrease in the amplitude of the observed drift of the measured values of G (which was mentioned above and also discussed elsewhere [12]) to a level of 0.01% of the baseline value may be a suitable design criterium for establishing the proper efficiency of the damping system.

Acknowledgement

The authors thank the State Committee for Science and Technologies of Russia, and the General Director of TRIBOTECH Research and Development Company, Mr. B.M. Krivitsky, for financial support of this work. We also thank N.I. Kolosnitsyn for assistance in the preparation of this manuscript.

References

- [1] G.T. Gillies, *Rep. Prog. Phys.* **60**, 151 (1997).
- [2] E.R. Cohen and B.N. Taylor, *Rev. Mod. Phys.* **59**, 1121 (1987).
- [3] G.G. Luther and W.R. Towler, *Phys. Rev. Lett.* **48**, 121 (1982).
- [4] C. Pontikis, *C. R. Acad. Sci. (Paris)* **274**, 437 (1972).
- [5] M.U. Sagitov, V.K. Milyukov, Y.A. Monakhov, V.S. Nazarenko and K.G. Tadzhdinov, *Dokl. Akad. Nauk SSSR, Earth Sciences* **245**, 567 (1979).
- [6] M.P. Fitzgerald and T.R. Armstrong, *IEEE Trans. Instrum. Meas.* **44**, 494 (1995).
- [7] W. Michaelis, H. Haars and R. Augustin, *Metrologia* **32**, 267 (1995/96).
- [8] H. Walesch, H. Meyer, H. Piel and J. Schurr, *IEEE Trans. Instrum. Meas.* **44**, 491 (1995).
- [9] B. Hubler, A. Cornaz and W. Kundig, *Phys. Rev. D* **51**, 4005 (1995).
- [10] C.H. Bagley and G.G. Luther, *Phys. Rev. Lett.* **78**, 3047 (1997).
- [11] O.V. Karagioz, V.P. Izmaylov, A.A. Silin and E.A. Dukhovskoy, in: "Universal Gravitation and the Theory of Space-Time", People's Friendship University Publishers, Moscow, 1987, pp. 102-110 (in Russian).
- [12] V.P. Izmaylov, O.V. Karagioz, V.A. Kuznetsov, V.N. Melnikov and A.E. Roslyakov, *Measurement Techniques* **36**, 1065 (1993) (translated from *Izmeritel'naya Tekhnika*, Russia).
- [13] O.V. Karagioz and V.P. Izmailov, *Measurement Techniques* **39**, 979 (1996) (translated from *Izmeritel'naya Tekhnika*, Russia).
- [14] N.I. Agafonov, V.V. Voronkov, V.P. Izmaylov and O.V. Karagioz, in: "Problems of Gravitational Measurements. Experimental Physics". Series B (VNIIOFI, Moscow, 1971), Vol. 1, pp. 151-165.
- [15] O.V. Karagioz, V.P. Izmaylov, N.I. Agafonov, E.G. Kocheryan and Yu.A. Tarakonov, *Izv. Akad. Nauk. SSSR, Fizika Zemli*, **12**, 106 (1976).
- [16] O.V. Karagioz, V.P. Izmaylov and A.I. Kuznetsov, *Vestnik Mosk. Univ., Ser. Geod. Aerofotog.*, No. 3, 91 (1992).
- [17] D.R. Long, *Nature* **260**, 417 (1970).

